Eur. J. Mineral.
2003, **15**, 965–975

Highly magnesian olivines and green-core clinopyroxenes in ultrapotassic lavas from western Yunnan, China: evidence for a complex hybrid origin

YIGANG XU[1]*, XIAOLONG HUANG[1], MARTIN A. MENZIES[2] and RUCHENG WANG[3]

[1] Guangzhou Institute of Geochemistry, Chinese Academy of Sciences, 510640 Guangzhou, China
* Corresponding author: e-mail: yigangxu@gig.ac.cn
[2] Geology Department, Royal Holloway University of London, Egham, UK
[3] Department of Earth Sciences, Nanjing University, 210093 Nanjing, China

Abstract: Oligocene ultrapotassic rocks from western Yunnan have abundant olivines of varying size and green-core clinopyroxenes. Olivine macrocrysts (1-5 mm) have very high forsterite contents (Fo_{92-94}), and high CaO (0.15-0.30 wt%) and Cr_2O_3 (up to 0.23 wt%) contents. They are believed to be magmatic rather than disintegrated crystals from the upper mantle. These magnesian olivines are not in equilibrium with melts corresponding to the whole-rock compositions of host lavas and, as such, may represent xenocrysts entrained by ultrapotassic magmas during their ascent to the surface. While komaiites, boninites and olivine lamproites are potential sources of these xenocrysts, a genetic link to the late Permian Emeishan large igneous province (LIP) is favoured, because the Emeishan flood basalt is the only known geologic event in the studied area that could have produced highly magnesian olivines. The olivine xenocrysts may have been entrained from the high velocity lower crust (Vp = 7.1-7.8 km/s), which is believed to have formed from high Mg basalts (picrites?) that underplated and intruded the crust during the Emeishan flood basalt episode. Given the presence of olivine xenocrysts and reverse-zoned clinopyroxenes, it is apparent that some magnesian ultrapotassic lavas from Yunnan have a complex hybrid origin. While the former point to ultramafic/primary melts the latter indicate interaction between evolved melts and relatively primary melts thus indicating complex magma mixing processes.

Key-words: magnesian olivine, green-core clinopyroxene, ultrapotassic lavas, Yunnan.

Introduction

Highly magnesian olivines are of great importance in igneous petrology and mantle geodynamics because they provide information about the nature of primary melts and melting mechanisms in the deep mantle. Magnesian olivines (Fo_{93-94}) occur in high-temperature volcanic rocks like komatiites and picrites (Nisbet *et al.*, 1993; Francis, 1985; Thompson & Gibson, 2000; Larsen & Pedersen, 2000) and in boninites and olivine lamproites that are derived from refractory mantle sources (Crawford, 1989; Jaques *et al.*, 1984; Mitchell & Bergman, 1991). Another occurrence of magnesian olivines is in refractory mantle peridotites produced by melt extraction processes perhaps modified by melt interaction (Bernstein *et al.*, 1998, and references therein). Therefore, magnesian olivines may either crystallize from ultramafic melts or represent disintegrated depleted mantle left by the extraction of komaiitic magmas. In this paper, we document highly magnesian olivines (Fo_{93-94}) in Oligocene ultrapotassic rocks from western Yunnan (Xie *et al.*, 1995; Xu *et al.*, 2001b). Such olivines are unusual in such a host rock where the reported compositions are generally less magnesian (Fo_{90-91}) (*e.g.*, Kamenetsky *et al.*, 1995). In addition, green-core clinopyroxenes are also present in some samples. In order to elucidate the petrogenetic significance of these minerals, detailed petrographic and mineral chemistry analyses have been performed on four samples of ultrapotassic volcanic rock from Yunnan. The aims of this paper are:

(a) to establish the origin of the highly magnesian olivines and green-core clinopyroxenes (*e.g.*, cognate phenocryts, xenocrysts) and the relationship to the host magma (*i.e.*, equilibrium/disequilibrium);
(b) to evaluate the provenance of magnesian olivines in terms of the regional crust-mantle geodynamics, and
(c) to constrain the magmatic evolution (magma mixing and fractionation) of the ultrapotassic melts on the basis of their mineralogy.

Geological setting and previous studies

The Ailao Shan-Red River (ASRR) fault is a major sinistral strike-slip fault in SW China (Fig. 1). Sinistral movement along this fault has displaced the Indochina block to the southeast (Tapponnier *et al.*, 1982) by some 500-700 km (Leloup *et al.*, 1995; Chung *et al.*, 1997). This fault is also considered as a suture zone which separates the Yangtze cra-

0935-1221/03/0015-0965 $ 4.95
DOI: 10.1127/0935-1221/2003/0015-0965

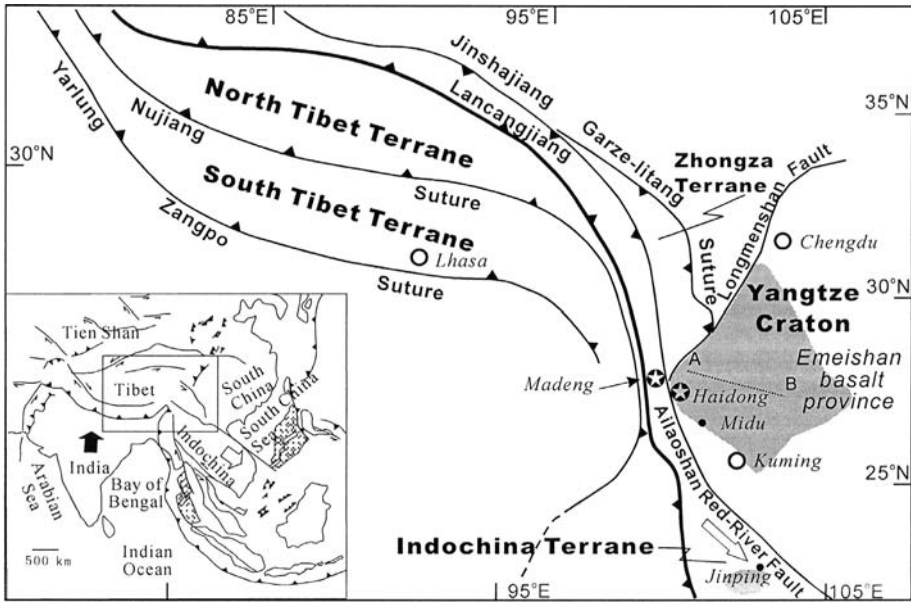

Fig. 1. Sketch map showing the major tectonic units of SW China and location of the studied ultrapotassic rocks. Shaded areas marked the late Permian Emeishan flood basalt province in western Yangtze craton. The line A-B shows the position of seismic transect across the Emeishan large igneous province (see Fig. 9a).

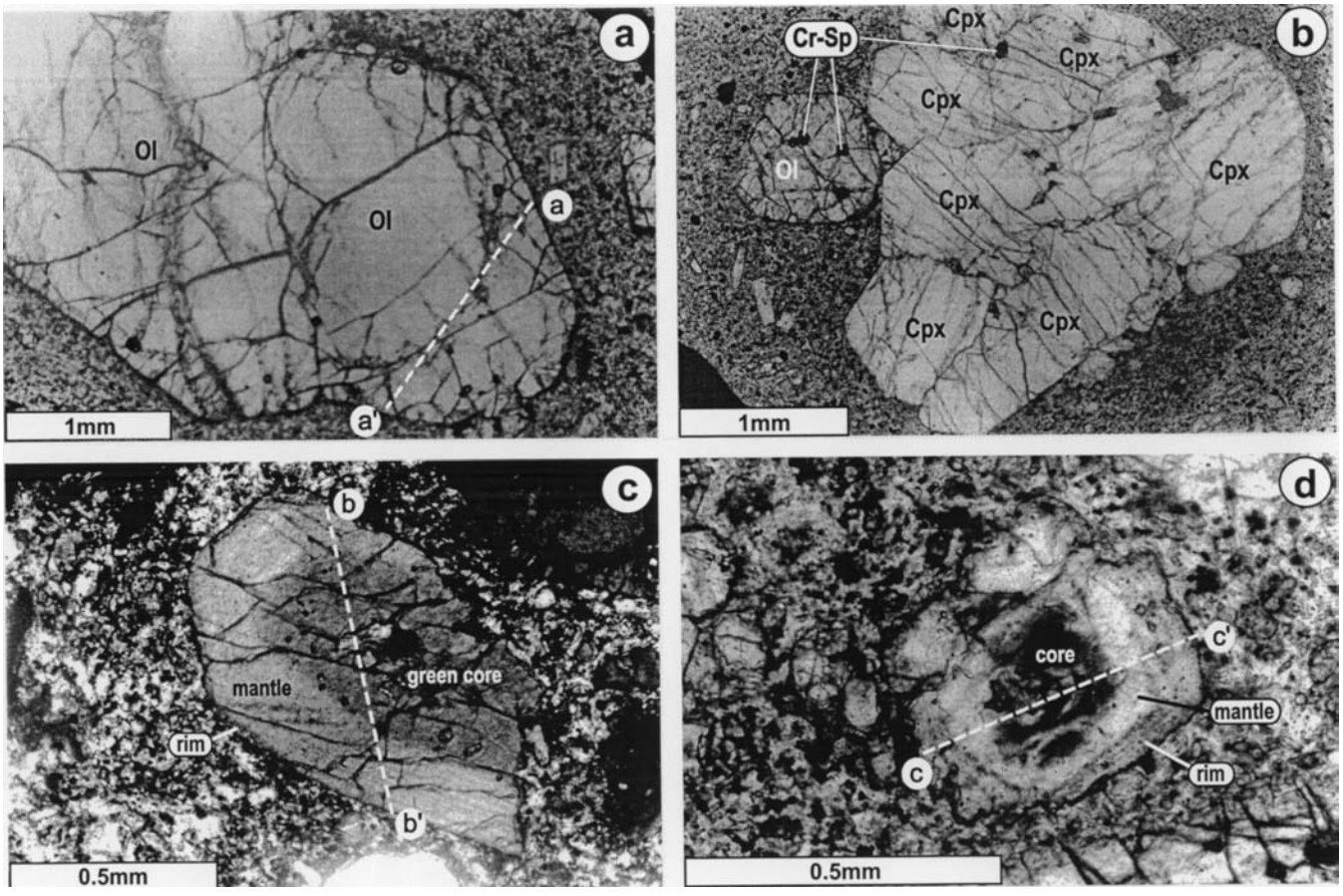

Fig. 2. Photomicrographs of the Oligocene ultrapotassic lavas from western Yunnan. (a) Microcrysts of olivine in a fine-grained matrix (YBW-9); (b) Clinopyroxene aggregates in sample YBW-10. Note the small chromite inclusions in subhedral olivine; (c) Partially resorbed clinopyroxene phenocryst with green core; (d) Clinopyroxene phenocryst with irregular core, colorless mantle and light brown rim. Dashed lines (a-a', b-b' and c-c') mark the traverse analyses by electron microprobe.

ton and Sanjiang Palaeo-Tethys region (Wang *et al.*, 2000). Oligocene volcanic lavas occur sporadically along the ASRR fault zone and some of them (*i.e.*, Haidong) were erupted through the late Permian Emeishan flood basalts (2.5×10^5 km^2), western Yangtze (Chung *et al.*, 1998a). Most of these lavas have high K_2O content (up to 6.5 wt%) and high K_2O/Na_2O ratio (>2), and are classified as ultrapotassic rocks (Xu *et al.*, 2001b). They are characterized by

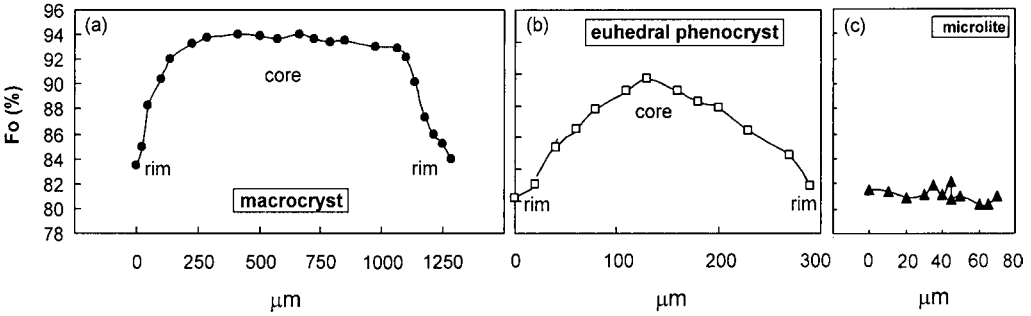

Fig. 3. Microprobe traverse across olivine crystals in sample YBW-9. (a) macrocryst (line a-a' in Fig. 2a); (b) euhedral phenocryst and (c) microlite.

high MgO (up to 17%) and uniformly low TiO_2 (<0.7 wt%) and P_2O_5 contents (<0.5 wt%). Trace element and isotope compositions suggest a subduction-modified mantle source for these K-rich lavas (Chung *et al.*, 1998b; Xu *et al.*, 2001b). Although the generation of potassic rocks are traditionally considered as a result of convective thinning of lithosphere after continental collision (Chung *et al.*, 1998b), Xu *et al.* (2001b) suggested that potassic magmatism may be related to lithospheric extrusion due to the Indo-Euroasian collision. While previous studies concentrated on whole rock geochemistry, mineralogy and mineral chemistry are the subject of this study.

Petrographic observation

The ultrapotassic lavas from Midu (Fig. 1) range from subaphyric to moderately porphyritic and the dominant phenocrysts are clinopyroxene, phlogopite and K-feldspar. No olivines have been observed in these lavas. The groundmass is composed of clinopyroxene, plagioclase, biotite and occasional magnetite. MgO contents can be as high as 16 wt% (Xu *et al.*, 2001b). In contrast, the magnesian samples from Madeng and Haidong are strongly porphyritic with phenocryst contents ranging from 10 to 40%. The phenocryst assemblage in these lavas consists of dominant olivine and variable amounts of clinopyroxene + K-feldspar ± phlogopite aggregates (Fig. 2a, b). The variable phenocryst content reveals that these Mg-rich lavas are not liquidus melts but may be modified by cumulus processes. Olivine crystals in the Madeng samples are very abundant (> 20%) and vary in size from 1 to 5 mm. These large olivines are termed "macrocrysts" and are free of deformation and spinel inclusions. Some of them are partially serpentinized. No euhedral olivine phenocrysts and microlites are found in the Madeng samples.

In contrast, olivines in the Haidong samples vary considerably in grain-size (<0.1 to 2 mm). In addition to the "macrocrysts" (1-2 mm) which are petrographically similar to those in the Madeng samples, euhedral-subhedral olivines and matrix olivines are also observed in the Haidong samples. Small chromites (± magnetite) occur as inclusions (<100 μm) in some euhedral-subhedral olivine phenocrysts (0.1-0.4 mm; Fig. 2b). Most clinopyroxene phenocrysts (<0.8 mm) are pale-green or colorless. Sample YBW-9 contains partially resorbed green-core clinopyroxene, surrounded by colorless mantles and light brown rims (Fig. 2c, d). The matrix contains microcrystals of the same mineral assemblage that occurs as phenocrysts together with minor Fe-Ti oxides. In this paper, focus will be placed on the compositions of diverse olivine phenocrysts and green-core clinopyroxene in the samples from Madeng (YJX-29, YJX-30) and Haidong (YBW-9, YBW-10).

Mineral chemistry

The mineral chemistry was obtained with a JOEL Superprobe at University of Nanjing, with crystal spectroscopy. Accelerating voltage was 15 kV, beam current 15 nA and beam diameter about 2 μm. The counting time varied between 10 and 30 s for different elements with 30 s for Ca analyses in olivine. Representative analyses are reported in Tables 1 to 3.

Olivine

The olivines in the Haidong samples span a wide compositional range (Fo_{94-79}) which is somewhat correlated with their size and crystal shape. The most magnesian contents (Fo_{92-94}) are found as "macrocrysts" (>1 mm). They have a flat compositional profile (Fo_{93-94}) in the central part of the crystal and show a steep compositional gradient towards the rim ($Fo_{83-84,}$ Fig. 3a). These high Fo olivines have high CaO content (0.1-0.3 wt%), compared to olivines observed in mantle xenoliths and orogenic peridotites which typically contain less than 0.1 wt% CaO (Simkin & Smith, 1978; Gurenko *et al.*, 1996; Fig. 4a). Although variable, Cr_2O_3 in these Mg-rich olivines (0.05 to 0.25 wt% with an average of 0.15 wt%) are considerably higher than the compositional range for typical mantle olivines, but are similar to those for olivines in boninites and picrites (Crawford, 1980; Thompson & Gibson, 2000).

The cores of euhedral olivines (0.1-0.3 mm) have slightly lower Fo ($Fo_{89-91.6}$) compared to those of "macrocrysts". The euhedral olivines are normally zoned with linear compositional gradients towards the margins (Fo_{83-84}, Fig. 3b). Unlike the "macrocrysts", these olivines lack homogeneous cores. Smaller olivines (<0.1 mm) and microlites have a more iron-rich composition (Fo_{79-82}), similar to the rim of large olivines. Relative to the "macrocrysts" they show higher contents of CaO and MnO and lower Cr_2O_3 (Fig. 4). CaO contents increase with decreasing Fo, a trend that is

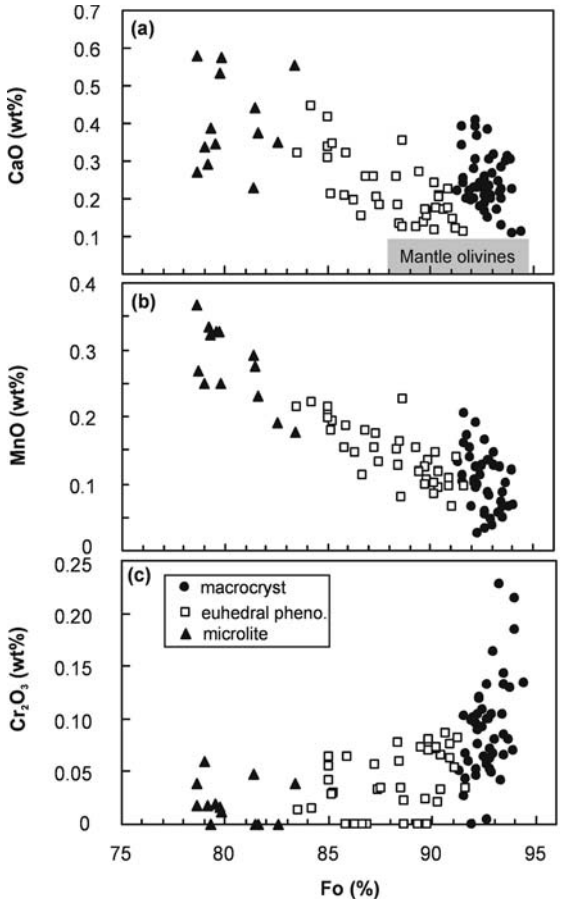

Fig. 4. CaO, MnO and Cr_2O_3 contents against Mg# of olivine in the Yunnan ultrapotassic lavas. The fields of mantle olivines are from Gurenko *et al.* (1996).

consistent with experimental predictions (Jurewicz & Watson 1988). Jurewicz & Watson (1988) experimentally demonstrated that the Ca content of an equilibrated olivine is chiefly dependent on both CaO and FeO content of the melt, rather than on pressure as previously thought (*e.g.*, Simkin & Smith, 1970). High FeO values result in olivines with higher CaO contents. Overall, the compositional trend defined by the euhedral phenocrysts and microlites is slightly different from that for the macrocrysts (Fig. 4).

Olivines in the Madeng samples show a limited compositional range as they occur only as "macrocrysts" (Table 1). The pattern of compositional zoning in the Madeng olivines is similar to that observed in the "macrocrysts" from Haidong, except that the rims have relatively higher Fo contents (Fo_{89-90}).

Chromite

Chromite inclusions in euhedral olivine phenocrysts are characterized by high Cr# varying from 0.79 to 0.87 and low Mg# (0.30-0.47). Coupled chromites and host olivines lie near the mantle array defined by Arai (1994a) (Fig. 5). TiO_2 content in chromite is generally low (<0.5 wt%), consistent with the low TiO_2 characteristics of the ultrapotassic magma system (Xu *et al.*, 2001b). Rare chromites have been detected by microprobe analyses in groundmass and show lower $Fe^{3+}/(Al+Fe^{3+}+Cr)$ ratios and Ti contents relative to the chromite inclusions in magnesian olivines (Table 3).

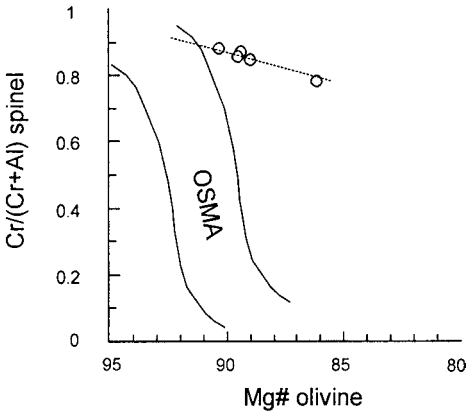

Fig. 5. Relationship between Fo of olivine and Cr# of chromite included in olivines in the Yunnan potassic lavas. The olivine-spinel mantle array (OSMA) is defined by Arai (1994a).

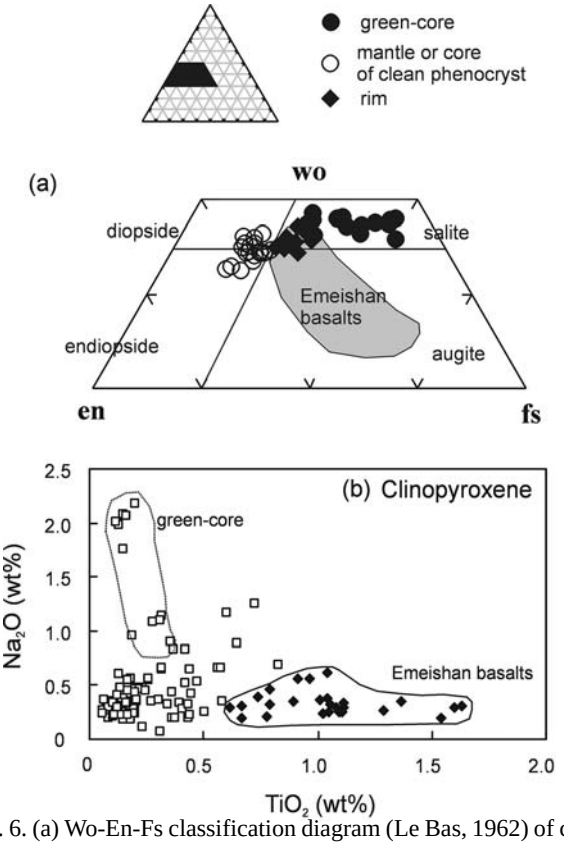

Fig. 6. (a) Wo-En-Fs classification diagram (Le Bas, 1962) of clinopyroxene from the Yunnan ultrapotassic rocks. (b) Na_2O contents in clinopyroxene against TiO_2. Composition of clinopyroxenes in the Emeishan flood basalts (Y.G. Xu, unpublished data) is shown for comparison.

Clinopyroxene

The pale green and colorless clinopyroxene phenocrysts are Ti-Al-poor diopside (Fig. 6a). They contain 0.06-0.4 wt%

Table 1. Representative analyses of olivines from Yunnan ultrapotassic rocks.

	YBW-9					YBW-10					YJX-29		YJX-30	
	macrocryst		euhedral pheno.		microlite	macrocryst		euhedral pheno.		microlite	macrocryst		macrocryst	
	core	rim	core	rim		core	rim	core	rim		core	rim	core	rim
SiO_2	41.53	40.47	41.07	39.76	39.03	42.03	39.07	40.56	39.56	38.89	41.90	41.27	41.22	39.21
TiO_2	0.01	0.03	0.00	0.04	0.02	0.00	0.00	0.03	0.00	0.00	0.00	0.00	0.00	0.00
Al_2O_3	0.01	0.00	0.03	0.00	0.00	0.01	0.00	0.04	0.00	0.01	0.03	0.03	0.11	0.05
Cr_2O_3	0.13	0.03	0.06	0.02	0.00	0.12	0.01	0.02	0.00	0.02	0.18	0.03	0.08	0.05
FeO	6.12	13.81	8.85	14.68	17.09	6.83	17.30	9.54	16.36	18.87	6.00	8.21	7.02	9.18
MnO	0.07	0.19	0.11	0.22	0.27	0.00	0.00	0.15	0.19	0.33	0.12	0.11	0.09	0.05
NiO	0.21	0.11	0.18	0.07	0.06	0.18	0.07	0.30	0.13	0.02	0.20	0.16	0.52	0.34
MgO	51.42	44.34	48.99	43.47	41.78	51.34	42.47	49.19	43.04	40.80	51.85	49.44	50.08	50.97
CaO	0.21	0.35	0.18	0.45	0.44	0.15	0.22	0.18	0.35	0.35	0.22	0.39	0.15	0.33
Na_2O	0.03	0.00	0.02	0.05	0.00	0.01	0.02	0.03	0.00	0.00	0.03	0.01	0.02	0.03
K_2O	0.02	0.00	0.01	0.00	0.01	0.00	0.01	0.01	0.01	0.02	0.01	0.00	0.01	0.00
Total	99.76	99.69	99.70	99.20	99.18	100.68	99.17	100.07	99.64	99.30	100.54	99.64	99.30	100.20
Cations per 4 oxygens														
Si	1.004	1.016	1.007	1.010	1.004	1.008	1.000	0.994	1.004	1.003	1.004	1.008	1.006	0.963
Ti	0.000	0.001	0.000	0.001	0.000	0.000	0.000	0.000	0.000	0.000	0.000	0.000	0.000	0.000
Al	0.000	0.000	0.001	0.000	0.000	0.000	0.000	0.001	0.000	0.000	0.001	0.001	0.003	0.002
Cr	0.002	0.001	0.001	0.000	0.000	0.002	0.000	0.000	0.000	0.000	0.003	0.001	0.002	0.001
Fe	0.124	0.290	0.181	0.312	0.368	0.137	0.370	0.196	0.347	0.407	0.120	0.168	0.143	0.188
Mn	0.001	0.004	0.002	0.005	0.006	0.000	0.000	0.003	0.004	0.007	0.002	0.002	0.002	0.001
Ni	0.004	0.002	0.004	0.001	0.001	0.004	0.001	0.006	0.003	0.000	0.004	0.003	0.010	0.007
Mg	1.852	1.660	1.790	1.646	1.603	1.836	1.621	1.798	1.628	1.569	1.853	1.799	1.822	1.866
Ca	0.005	0.009	0.005	0.012	0.012	0.004	0.006	0.005	0.010	0.010	0.006	0.010	0.004	0.009
Na	0.001	0.000	0.001	0.003	0.000	0.000	0.001	0.001	0.000	0.000	0.001	0.000	0.001	0.001
K	0.001	0.000	0.000	0.000	0.000	0.000	0.000	0.000	0.000	0.001	0.000	0.000	0.000	0.000
Mg#	93.7	85.1	90.8	84.1	81.3	93.1	81.4	90.2	82.4	79.4	93.9	91.5	92.7	90.8

TiO_2, 1.2-1.5 wt% Al_2O_3, 0-0.8 wt% Cr_2O_3 and 0.3-0.4 wt% Na_2O (Table 2). They are normally zoned with Mg-rich cores (Mg# = 0.89) and Fe-rich rims (Mg# = 0.82).

More complex zoning patterns are observed in clinopyroxenes with green cores. Fig. 7 shows a microprobe traverse of two green-core clinopyroxenes. The green cores are relatively rich in FeO, Al_2O_3 and Na_2O (Mg# = 0.65-0.75, Al_2O_3 = 2.8-4.4 wt%, Na_2O = 1-2.2 wt%, Table 2), similar to those known in literature as salite (*e.g.*, Duda & Schmincke, 1985; Fig. 6a). Like the dominant diopsides, the salites in the Yunnan ultrapotassic rocks show low TiO_2 (0.2-0.3 wt%) contents (Fig. 6b). This is distinct from diopsides found in alkaline mafic basalts and flood basalts, which are generally higher in Al and Ti contents (Wass, 1979; Fig. 6b). One clinopyroxene grain shows an oscillatory-zoned core with a sharp transition in composition from salite to diopside (Mg# = 0.86-0.89). The latter is compositionally similar to the dominant diopside phenocrysts and shows a normal zoning with Mg# of 0.81 towards the rim (Fig. 7).

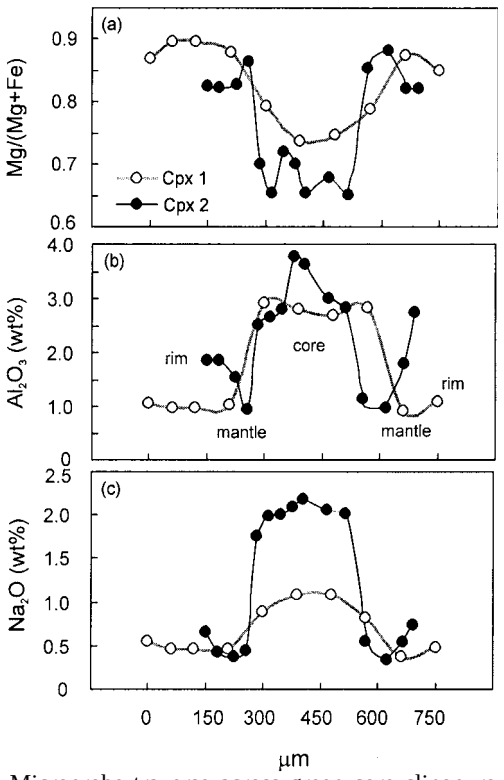

Fig. 7. Microprobe traverse across green core clinopyroxene. (a) Mg#; (b) Al_2O_3 and (c) Na_2O. Cpx-1: line b-b' in Fig. 2c; Cpx-2: line c-c' in Fig. 2d.

Feldspar, biotite and magnetite

Alkali feldspar in the Yunnan potassic rocks shows a restricted compositional range ($An_{3-8}Ab_{31-39}Or_{55-66}$). Mica is only occasionally found in the Madeng and Haidong samples (Table 3) and is characterized by lower TiO_2 and higher Al_2O_3 contents than those shown by typical lamproitic

Table 2. Representative analyses of clinopyroxenes from Yunnan ultrapotassic rocks.

	YBW-9								YBW-10		YJX-29		YJX-30	
	Cpx-1			Cpx-2			phenocryst		phenocryst		phenocryst		phenocryst	
	green-core	mantle	rim	green-core	mantle	rim	core	rim	core	rim	core	rim	core	rim
SiO_2	51.74	53.92	54.32	52.80	53.97	52.66	53.73	52.28	52.80	51.97	53.69	51.23	53.11	51.87
TiO_2	0.31	0.22	0.14	0.20	0.16	0.45	0.18	0.32	0.06	0.20	0.10	0.44	0.06	0.23
Al_2O_3	2.80	0.97	1.08	3.63	0.86	1.86	1.16	1.61	1.39	1.40	1.54	2.47	1.35	1.61
Cr_2O_3	0.00	1.22	0.00	0.01	0.54	0.09	0.00	0.18	0.42	0.22	0.84	0.30	0.76	0.12
FeO	8.11	3.47	5.44	9.75	4.27	6.23	4.39	5.98	4.01	5.35	3.66	6.27	3.52	6.13
MnO	0.25	0.13	0.19	0.30	0.15	0.20	0.18	0.12	0.06	0.00	0.09	0.11	0.15	0.00
NiO	0.01	0.01	0.01	0.00	0.02	0.00	0.00	0.09	0.00	0.12	0.05	0.00	0.09	0.07
MgO	12.67	16.85	17.04	10.25	17.43	15.95	17.40	16.40	16.83	16.71	17.17	14.66	18.42	17.61
CaO	22.42	22.57	21.58	19.99	22.09	22.20	22.37	22.52	22.16	21.36	22.31	22.75	21.67	21.73
Na_2O	1.09	0.47	0.48	2.17	0.34	0.42	0.43	0.65	0.27	0.29	0.34	0.19	0.23	0.11
K_2O	0.01	0.00	0.00	0.08	0.00	0.01	0.02	0.01	0.05	0.05	0.01	0.01	0.03	0.00
Total	99.41	99.84	100.30	99.18	99.83	100.06	99.87	100.15	98.03	97.68	99.79	98.43	99.39	99.48
Cations per 6 oxygens														
Si	1.942	1.971	1.981	1.985	1.974	1.942	1.966	1.931	1.966	1.953	1.961	1.926	1.947	1.922
Ti	0.009	0.006	0.004	0.006	0.004	0.012	0.005	0.009	0.002	0.006	0.003	0.012	0.002	0.007
Al	0.124	0.042	0.047	0.161	0.037	0.081	0.050	0.070	0.061	0.062	0.066	0.109	0.058	0.070
Cr	0.000	0.035	0.000	0.000	0.016	0.003	0.000	0.005	0.012	0.007	0.024	0.009	0.022	0.003
Fe	0.255	0.106	0.166	0.306	0.131	0.192	0.134	0.185	0.125	0.168	0.112	0.197	0.108	0.190
Mn	0.008	0.004	0.006	0.010	0.005	0.006	0.006	0.004	0.002	0.000	0.003	0.004	0.005	0.000
Ni	0.000	0.000	0.000	0.000	0.001	0.000	0.000	0.003	0.000	0.004	0.001	0.000	0.003	0.002
Mg	0.709	0.919	0.927	0.574	0.951	0.876	0.949	0.903	0.934	0.936	0.935	0.822	1.007	0.973
Ca	0.901	0.884	0.844	0.805	0.866	0.877	0.877	0.891	0.884	0.860	0.873	0.917	0.851	0.863
Na	0.079	0.033	0.034	0.158	0.024	0.030	0.030	0.046	0.019	0.021	0.024	0.014	0.017	0.008
K	0.000	0.000	0.000	0.004	0.000	0.000	0.001	0.000	0.002	0.002	0.000	0.000	0.001	0.000
Mg#	73.6	89.6	84.8	65.2	87.9	82.0	87.6	83.0	88.2	84.8	89.3	80.7	90.3	83.7

phlogopites (Mitchell & Bergman, 1991). Instead its composition resembles that of micas from shoshonitic lamprophyres.

Magnetites included in olivines generally have higher Cr_2O_3 content (up to 2.4 wt%) than in groundmass (< 0.1 wt%). This may suggest that Cr-rich magnetites crystallized as early as olivines, whereas the Cr-free magnetite crystallized in the late stage of magma evolution. Magnetite inclusions show lower ulvospinel content (Usp_{6-11}) than those in the groundmass (Usp_{31-39}, Table 3).

Discussion

A. Origin of highly magnesian olivines and geodynamic implications

Magnesian olivines (Fo_{90-91}) have been documented in potassic and ultrapotassic rocks around the world (*e.g.*, Barton & van Bergen, 1981; Mitchell & Bergman, 1991; Kamentsky *et al.*, 1995; Di Battistini *et al.*, 1998). Relatively high CaO contents (>0.2 wt%) make many authors consider most of these olivines to be a near-primary assemblage in equilibrium with mantle peridotites that crystallized at the onset of magmatic differentiation (Kamentsky *et al.*, 1995; Di Battistini *et al.*, 1998). The "macrocrysts" of olivines in the Yunnan ultrapotassic rocks have higher CaO and Cr_2O_3 contents than typical mantle olivines (Fig. 4). They have relatively low NiO contents compared to the mantle olivine array defined by Takahashi *et al.* (1987). Similar low NiO content has been documented in olivines from some cumulate ultramafic complexes (*e.g.*, Takahashi *et al.*, 1991). Accordingly, the macrocrysts of olivines are believed to be magmatic rather than disintegrated crystals from the upper mantle. One may thus argue that the olivine "macrocrysts" could be genetically related to potassic magmatism, that is, they are crystallized phases from primary lavas that formed on the floors of magma chamber or magmatic conduit walls.

To evaluate this possibility, the composition of olivines in the Yunnan ultrapotassic rocks is compared with their whole rock chemistry in Fig. 8a. The curve in Fig. 8a shows the variation in olivine composition in equilibrium with melts that were not subjected to significant crystal fractionation or accumulation (Revillon *et al.*, 1999). The most magnesian ("cognate") olivine in a given lava in equilibrium with liquids should plot along this curve, whereas olivine crystallizing from differentiating magmas should plot below the curve. Xenolithic olivines could plot above or below the curve, depending upon the nature of their source (Revillon *et al.*, 1999). It is clear from Fig. 8a that the "macrocrysts" of olivine in the Yunnan ultrapotassic rocks are not in equilibrium with melts with the composition of the host rocks because most plot conspicuously above the equilibrium curve. These olivines are therefore believed to be xenocrystic in or-

Table 3. Representative analyses of spinel, magnetite, feldspar and biotite from Yunnan ultrapotassic rocks.

	Spinel			Magnetite			Feldspar				Biotite
sample	YBW-9	YBW-10	YJX-29	YBW-9	YBW-10	YJX-29	YBW-9	YBW-10	YJX-29	YJX-30	YBW-10
SiO_2	–	0.10	0.14	0.03	0.12	1.00	63.73	62.52	63.53	62.77	41.32
TiO_2	1.69	0.25	0.19	3.39	7.46	10.14	0.12	0.12	0.11	0.06	1.44
Al_2O_3	8.29	5.89	9.15	4.03	5.88	2.47	21.61	21.18	20.74	21.39	10.41
Cr_2O_3	35.76	62.70	58.00	2.43	1.12	0.08	–	0.03	0.00	0.34	0.19
FeO	46.68	19.98	22.50	81.65	76.34	74.04	0.40	0.39	0.40	0.48	6.93
MnO	0.34	0.44	0.62	0.34	0.47	0.62	0.09	0.05	0.01	0.03	0.07
NiO	0.06	0.18	0.08	0.15	0.05	0.07	–	0.04	0.01	–	0.01
MgO	6.65	10.84	8.87	3.14	3.11	1.53	0.00	–	0.07	0.03	27.18
CaO	–	0.02	0.01	–	–	1.15	0.56	1.17	0.88	1.07	0.05
Na_2O	0.07	–	–	–	0.09	0.15	4.33	4.47	3.89	3.39	0.41
K_2O	0.00	0.02	–	0.03	0.04	0.03	9.91	9.59	10.37	10.38	6.99
Total	99.54	100.40	99.56	95.17	94.67	91.27	100.76	99.55	99.99	99.93	95.00
Cations per formulate unit											
Si	–	0.003	0.005	0.001	0.004	0.038	2.862	2.838	2.882	2.860	2.979
Ti	0.043	0.006	0.005	0.093	0.204	0.294	0.004	0.004	0.004	0.002	0.078
Al	0.330	0.231	0.361	0.172	0.251	0.112	1.144	1.133	1.109	1.149	0.885
Cr	0.956	1.648	1.536	0.070	0.032	0.002	–	0.001	0.000	0.012	0.011
Fe	0.633	0.556	0.630	1.572	2.317	2.384	0.070	0.015	0.015	0.018	0.418
Mn	0.010	0.012	0.017	0.010	0.015	0.020	0.004	0.002	0.000	0.001	0.004
Ni	0.002	0.005	0.002	0.004	0.001	0.002	–	0.002	0.000	–	0.001
Mg	0.335	0.537	0.443	0.170	0.168	0.088	0.000	–	0.005	0.002	2.921
Ca	–	0.001	0.000	–	–	0.047	0.027	0.057	0.043	0.052	0.004
Na	0.005	–	–	–	0.006	0.011	0.377	0.393	0.342	0.300	0.057
K	0.000	0.001	–	0.001	0.002	0.002	0.568	0.555	0.600	0.604	0.643
O	4	4	4	4	4	4	8	8	8	8	11
Mg#	0.20	0.49	0.42								0.88
Cr#	0.74	0.88	0.81								
Usp				0.13	0.31	0.39					
An							0.03	0.06	0.04	0.05	
Ab							0.39	0.39	0.35	0.31	
Or							0.58	0.55	0.61	0.63	

igin. In contrast, the euhedral olivine phenocrysts plot along the equilibrium curve, suggesting their cognate affinity with the host lavas. Therefore, two genetically unrelated olivines are present in the Yunnan lavas. This is consistent with the fact that the olivine "macrocrysts" and euhedral phenocrysts do not show smooth and continuous compositional trends through the whole olivine compositional range (Fig. 4). It is also noted that olivine only occurs as xenolithic macrocrysts in the Madeng samples. Absence of euhedral olivine phenocrysts and microlites may suggest that olivine was not the liquidus phase in some potassic lavas. It follows that the magnesian olivine macrocrysts are xenocrysts, which were not genetically related to the potassic magmatism.

The zoning profile in the olivine crystals can be accounted for by re-equilibration by diffusional exchange between olivine and liquid (Maaloe & Hansen, 1982; Francis, 1985; Larsen & Pedersen, 2000). The degree of re-equilibration is clearly dependent on the size of olivine. The core-rim variation in Fo is more limited ($Fo_{94\text{-}90}$) in large olivine xenocrysts (> 4 mm, YJX-29) than in small xenocrysts (~1 mm; $Fo_{94\text{-}84}$, YBW-9). The similarity in core composition of olivines from different samples suggests that these grains may have the same origin.

The olivine xenocrysts in the Yunnan lavas have a very high forsterite content ($Fo_{93\text{-}94}$). Similarly high Fo olivine has been reported in komatiites and picrites (Nisbet *et al.*, 1993; Francis, 1985; Thompson & Gibson, 2000; Larsen & Pedersen, 2000), and in boninites and olivine lamproites (Crawford, 1989; Jaques *et al.*, 1984). These magmas should therefore be considered as potential sources for the olivine xenocrysts in the Yunnan lavas. Evaluation of these alternatives is not an easy task because we cannot date olivine. However, any model proposed for the origin of olivine xenocrysts must be consistent with geological and geophysical data. Komatiites are generally associated with the Archean terrain, but the Yangtze craton is Proterozoic (Yang *et al.*, 1986). In fact, komatiites are not known so far in the studied area. The very high Cr# and low Al_2O_3 of the Yunnan spinels and their magnesian host olivines (Fig. 5) are comparable to those of boninites. However, some Yunnan spinels have higher TiO_2 contents than those from boninites at given Al_2O_3 (Crawford, 1980; Walker & Cameron, 1983; see Table 3). Moreover, spinel inclusions occur in euhedral olivines but are not present in the olivine xenocrysts. It may be inadequate to use spinel compositions to constrain the or-

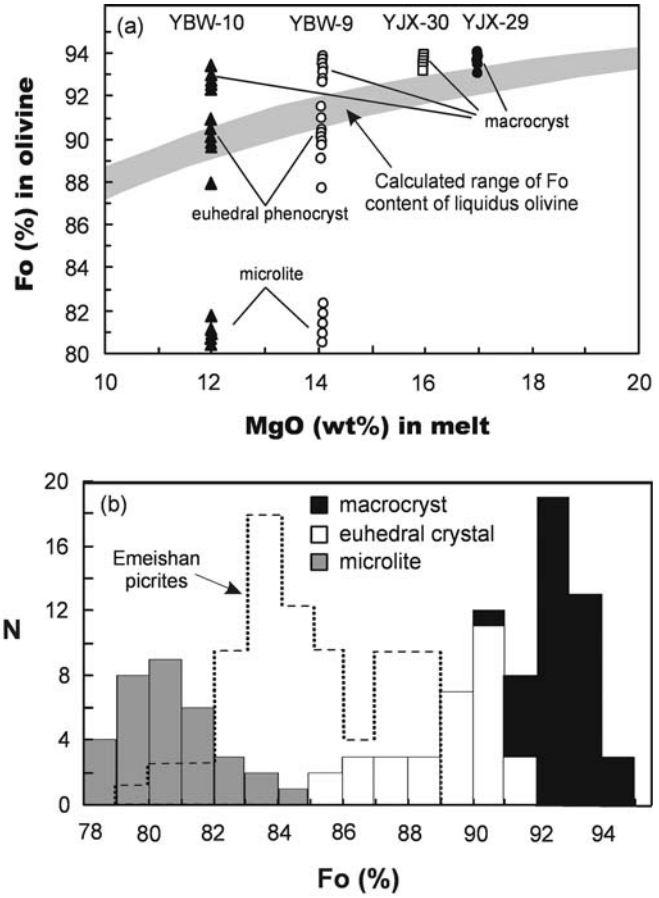

Fig. 8. (a) Comparison between the range of Fo in olivine phenocrysts in the Yunnan potassic rocks and corresponding whole rock MgO contents. The shaded area defines the range of olivine compositions calculated to be in equilibrium with each of the bulk-rock compositions. The partition coefficients of Fe-Mg between olivine and liquid are taken from Ulmer (1989). Bulk rock composition is after Xu *et al.* (2001b); (b) Comparison of composition of olivines in Yunnan potassic rocks and in picrites from the Late Permian Emeishan flood basalt province. Data for the Emeishan picrites are taken from Xu & Chung (2001) and Y.G. Xu (unpublished data).

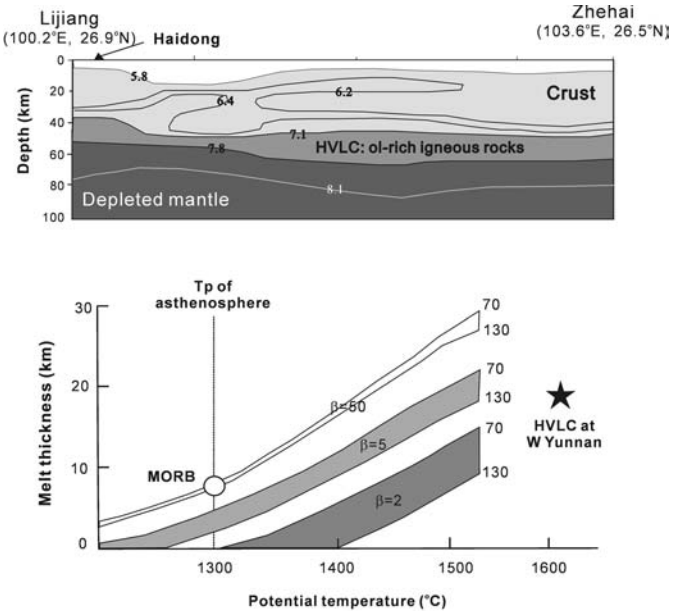

Fig. 9. A petrologic interpretation of seismic tomographic velocity structure of the lower crust beneath west Yangtze craton (modified after Liu *et al.*, 2001). Location of the seismic profile from Lijiang to Zhehai is shown in Fig. 1 (line A-B); (b) Variation of melt thickness as a function of potential temperature (Tp) and β for lithosphere ranging in thickness from 70 to 130 km (after White & McKenzie, 1989). The thick HVLC in the west Yangtze craton and a limited lithospheric extension suggest a high potential temperature for the mantle from which the materials in the HVLC were derived.

igin of olivine xenocrysts, because olivine xenocrysts and spinel included in euhedral olivines may represent the products of two unrelated magmatic suites. Another line of evidence against the boninite alternative is the lack of this magma type in the studied region.

Diamond prospecting during the late seventies and early eighties led to a detailed mineralogical and petrologic comparison between the Yunnan K-rich rocks and the olivine lamproites from western Australia. It has been shown that the Yunnan Cenozoic K-lavas are not the analogue of the Australian olivine lamproites (BGRY, 1990). The only known geological event in the studied area which could have produced highly magnesian picrites/basalts is the late Permian Emeishan large igneous province (LIP) believed to have formed as a result of plume impact on the base of the lithosphere (Chung *et al.*, 1998a; Xu *et al.*, 2001a). It is thus possible that the olivine xenocrysts in the Yunnan ultrapotassic lavas could be genetically related to the Emeishan flood basaltic volcanism. One may argue against this proposal given the contrasting compositions of olivine xenocrysts (Fo_{93-94}) in the Yunnan lavas and those in picrites recovered so far from the Emeishan LIP (Fo_{89}) (Fig. 8b). However, the lack of highly magnesian olivines in the Emeishan picrites may in part be due to insufficient analyses of picrite samples. Alternatively, the ultramafic melts that crystallized Fo_{92-94} olivines were too dense to arise through the thick continental crust and remain trapped at Moho depths (Cox, 1980). Recent seismic tomographic data reveal the presence of a thick (*ca.* 20 km) high velocity lower crust (HVLC) (Vp = 7.1-7.8 km/s) in the west Yangtze craton (Fig. 9a; Liu *et al.*, 2001). The HVLC is generally interpreted as mafic igneous rocks underplated at the Moho (White & McKenzie, 1989; Kelemen & Holbrook 1995; Farnetani *et al.*, 1996; Korenaga *et al.*, 2000). For instance, the high seismic velocity crust at the Namibian volcanic margin has been modelled as basaltic material with about 15% MgO (Trumbull *et al.*, 2002). The Vp of the HVLC in the west Yangtze craton varies from 7.1 to 7.8 km/s, significantly higher than gabbroic rocks in normal oceanic crust (Vp = 6.8 to 7.0 km/s.). This suggests a high proportion of olivine (and garnet) in the underplated igneous rocks. Possible olivine-rich igneous rocks include picrites, olivine gabbros and cumulate peridotites.

The formation of the HVLC may be in response to a deep-seated mantle plume (White & McKenzie, 1989) or associated with mantle upwelling (*e.g.*, Kelemen & Holbrook 1995). In the Yunnan case where lithospheric exten-

sion rate was low during the Permian period (*c.f.*, Thompson *et al.*, 2001), production of a thick magnesian basalt layer requires a mantle with potential temperature greater than 1600 °C (Fig. 9b). A high mantle potential temperature (> 1500 °C) has also been obtained from REE inversion of the low-Ti basalts from the Emeishan LIP (Xu *et al.*, 2001a). The REE inversion results further suggest that the total thickness of melts produced during the Emeishan basaltic magmatism is over 5 km (Xu *et al.*, 2001a). The discrepancy between this estimated thickness and the erupted thickness (~3 km) probably reflects that high-density lavas were underplated at the Moho or in the lowermost part of crust. Accordingly, we propose that the formation of the thick HVLC may be related to the Emeishan flood basalt event, although the age of the HVLC remains unknown. Disruption of the derivatives/cumulates from these magmas acts as a mechanism for the entrainment of the magnesian olivines in the ultrapotassic volcanic rocks. This is possible because the ultrapotassic lavas erupted through the Emeishan LIP (Fig. 1). This interpretation implies a correlation between the olivine xenocrysts and high temperature melts. This inference is consistent with the high Cr_2O_3 contents in olivine xenocrysts (up to 0.25 wt%, compared with <0.1 wt % in euhedral crystals; Fig. 4c). According to Li *et al.* (1995), such high Cr contents in olivine are indicative of high temperature of parental melts from which the olivines crystallized.

B. Primary melts and source materials of the ultrapotassic lavas

The presence of olivine xenocrysts suggests that the lavas from Madeng and Haidong are not representative of equilibrium melts, but are likely to represent mixtures of evolved magmas and cumulate crystals or xenocrysts. Basically, the composition of the primary magmas can be deduced by subtracting olivines (Fo_{92-94}) from the measured whole rock composition. However, this simple conclusion is negated by possible magma replenishment-mixing processes as suggested by the clinopyroxene composition (see next section). As discussed above, there are two genetically unrelated olivines in Yunnan ultrapotassic lavas. While high Fo "macrocrysts" are "exotic", euhedral phenocrysts may be "cognate" to the potassic magmas. Constraints on the nature of primary potassic melts may accordingly come from the earliest crystallized phases in the system. Petrographic observation and mineral chemistry suggest that the earliest crystallized phases are magnesian olivines (Fo_{89-91}) with chromite inclusions. These olivines were in equilibrium with magmas of Mg#=0.71-0.73 according to the Fe-Mg equilibrium coefficient (Ulmer 1989). The chromites and their host olivines are coupled in composition and form a Fo-Cr# fractionation line (Fig. 5). Extrapolation of this fractionation line back to the olivine-spinel mantle array suggests that they may have crystallized from very primitive liquids that could be in equilibrium with their mantle source (Arai, 1994b). The high Cr contents (Cr# up to 0.87) of chromite indicate that the parental melts came from a depleted mantle source (Arai, 1994b). This is consistent with the trace element composition which requires spinel harzburgite as the source for the Yunnan K-lavas (Xu *et al.*, 2001b). There is a general consensus that these potassic rocks derived from a subduction-modified, refractory lithospheric mantle. The harzburgitic composition of mantle source governs the major chemistry of the volcanic rocks, whereas the subduction-introduced components supply the bulk of incompatible and volatile elements.

The low ulvospinel content (Usp_{6-13}) in magnetites included in magnesian olivines may be suggestive of high f_{O2} in the source magmas, because ulvospinel content in magnetite is directly correlated with oxygen fugacity and temperature (Spence & Lindsley, 1981). Oxidation state of the source region may be related to percolation of slab-released fluids (Xu *et al.*, 2001b). Significantly high ulvospinel content (Usp_{31-39}) is found in magnetites in the groundmass, indicating a progressive decrease in f_{O2} during crystal fractionation. A similar evolution trend in oxygen fugacity has been noted for the potassic lavas from the Roman province (*e.g.*, Conticelli *et al.*, 1997).

C. Clinopyroxene zoning and magma chamber replenishment-mixing

The occurrence of resorbed green salites as cores in clinopyroxene phenocrysts has been widely reported in alkaline mafic to intermediate lavas (Wass, 1979; Duda & Schmincke, 1985; Neumann *et al.*, 1999), and potassic magmas (Di Battistini *et al.*, 1999). In general, green-core clinopyroxene is not in equilibrium with the host melts. This is also the case for the Yunnan lavas, as indicated by the coexistence of salite (Mg# = 0.65) and euhedral magnesian pyroxene (Mg# = 0.86-0.89) and olivine (Fo_{89-91}) phenocrysts. Two different petrogenetic models have been formulated to explain these disequilibrium assemblages and the origin of green-core clinopyroxene:

(a) Increasing oxygen and/or water fugacity as an explanation of cognate green-core clinopyroxenes with inverse zoning (Holm, 1982; Aurisicchio *et al.*, 1988);

(b) Magma mixing processes between variably evolved magmas as an explanation of the disequilibrium (Duda & Schmincke, 1985; Dobosi & Fodor, 1992; Neumann *et al.*, 1999). In this model, the green-core clinopyroxenes are regarded as xenocrysts. They may have been entrained from disintegrated wall rocks during magma ascent (Barton & van Bergen, 1981) or represent crystallization products of an evolved magma which subsequently mixed with a more primitive magma.

The relatively low mg-numbers (Mg# = 0.75-0.65) and high Na_2O in Yunnan salites are clearly not derived from the upper mantle. One could argue that green salites were extracted from crystal-plated conduits (Irving, 1980) formed in an early magmatic fractionation during the Emeishan basaltic magmatism. However, this possibility can be ruled out because the clinopyroxenes in the Emeishan lavas have higher TiO_2 and lower Na_2O compared to the salites in the ultrapotassic rocks (Fig. 6b). Low Ti content in the Yunnan salites mirrors that of the host rocks, probably suggesting a cognate origin of these crystals in the K-rich magmas.

The salite cores have lower MgO but higher Al_2O_3 (and higher Al^{VI}/Al^{IV}) than diopside rims. These may have crys-

tallized from evolved melts during earlier phases of potassic magmatism, but under higher pressures than diopside phenocrysts. The different compositions of the green-cores may record different evolutionary stages or suggest the involvement of different evolving magmas. The magnesian clinopyroxene surrounding green-cores can be accounted for by mixing of primitive magma with a pre-existing evolved magma that crystallized Na-salite, now present as cores. Resorbed or corroded cores to the salites may be the result of a temperature increase due to injection of fresh mafic magmas into the magma chamber. It is noted that the mantle-rim compositional variation (Mg# = 0.89 to 0.83) is similar to the normal zoning observed in many euhedral phenocrysts without green cores. This suggests that the clinopyroxene rim and the euhedral phenocrysts share a common parent (*i.e.* mafic magma) prior to the eruption of the host lavas.

Conclusions

(1) "Macrocrysts" of olivine in the Oligocene ultrapotassic rocks from western Yunnan are forsterite-rich (Fo_{92-94}). They are not in equilibrium with melts with the composition of the host rocks and are thus xenocrysts in origin. High CaO and Cr_2O_3 contents in high Fo_{92-94} olivines suggest that they do not represent disaggregated mantle peridotites but more likely crystallized from ultramafic melts. While komaiites, boninites and olivine lamproites are the potential sources of these xenocrysts, a genetic link to the late Permian Emeishan LIP is favoured on the basis of recent geological and geophysical data. Olivine xenocrysts may have been extracted from the high velocity lower crust, which is evident in seismic profiles. This HVLC is believed to have formed from high Mg basalts (picrites?) that underplated and intruded the crust during the Emeishan flood basalt volcanism.

(2) Given the presence of xenolithic olivines, some highly magnesian ultrapotassic rocks from Yunnan are not primary melts but are mixture of less mafic melts and olivine xenocryst. The composition of primitive magmas (Mg# = 0.71-0.73) is inferred from the compositions of early crystallized olivine (Fo_{89-91}) and included chromites (Cr# = 0.80-0.87), which in turn indicate a refractory harzburgitic source for the Yunnan ultrapotassic rocks.

(3) Complex compositional zoning in clinopyroxene phenocrysts provides information on magma evolution of the Yunnan ultrapotassic lavas. The green salite cores crystallized from evolving potassic magmas. The core development was followed by injection of more primitive liquid that crystallized euhedral diopside and clinopyroxenes surrounding green-cores. A likely scenario is the replenishment of a partially crystallization magma chamber by a mafic magma.

Acknowledgement: We thank S.L. Sha and G.H Xie for help in the field. Review comments of S. Foley and R. Altherr helped to improve the paper. The financial supports from the Chinese Academy of Sciences (KZCX2-209; KZCX2-101), the Chinese Ministry of Science and Technology (G1999043205) and the China National Science Foundation (40234046, 40202009, 49925308) are gratefully acknowledged. This represents part of a Chinese Academy of Sciences-Royal Society joint research project between the Institute of Geochemistry, Guangzhou (China) and the Department of Geology, Royal Holloway University of London (UK).

References

Arai, S. (1994a): Characterization of spinel peridotites by olivine-spinel compositional relationships: review and interpretation. *Chemical Geol.*, **113**, 191-204.

– (1994b): Compositional variation of olivine-chromian spinel in Mg-rich magmas as a guide to their residual spinel peridotites. *J. Volcanol. Geotherm. Res.*, **59**, 279-293.

Aurisicchio, C., Federico, M., Gianfagna, A. (1988): Clinopyroxene chemistry of the high potassium suite from Alban hills, Italy. *Contrib. Mineral. Petrol.*, **89**, 1-19.

Barton, M. & Bergen, v. M. J. (1981): Green clinopyroxenes and associated phases in a potassium-rich lava from the Leucite Hill, Wyoming. *Contrib. Mineral. Petrol.*, **77**, 101-114.

Bernstein, S., Kelemen, P.B., Brooks, C.K. (1998): Depleted spinel harzburgite xenoliths in Tertiary dykes from East Greenland: Restites from high degree melting. *Earth Planet. Sci. Lett.*, **154**, 221-235.

Boyd, F.R. (1989): Compositional distinction between oceanic and cratonic lithosphere. *Earth Planet. Sci. Lett.*, **96**, 15-26.

BGRY (Bureau of Geology and Resources of Yunnan Province) (1990): "Regional geology of Yunnan province". Geol. Mem. Series 21, Geologic Press, Beijing, 728 pp (in Chinese).

Chung, S.L., Lee, T.Y., Lo, C.H., Wang, P.L., Chen, C.Y., Nguyen, T.Y., Tran, T.H., Wu, G.Y. (1997): Intraplate extension prior to continental extrusion along the Ailao Shan-Red River shear zone. *Geology*, **25**, 311-314.

Chung, S.L., Jahn, B.M., Wu, G.Y., Lo, C.H., Cong, B.L. (1998a): The Emeishan flood basalt in SW China: A mantle plume initiation model and its connection with continental break-up and mass extinction at the Permian-Triassic boundary. *In* "Mantle dynamics and plate interaction in East Asia", M.F.J. Flower, S.L. Chung, C.H. Lo, T.Y. Li, eds., American Geophysical Union Geodynamic Series, **27**, 47-58.

Chung, S.L., Lo, C.H., Lee, T.Y., Zhang, Y., Xie, Y., Li, X.H., Wang, K.L., Wang, P.L. (1998b): Diachronous uplift of the Tibetan Plateau starting 40 Myr ago. *Nature*, **394**, 769-773.

Conticelli, S., Francalanci, L., Manetti, P., Cioni, R., Sbrana, A. (1997): Petrology and geochemistry of the ultrapotassic rocks from the Sabatni Volcanic District, central Italy: the role of evolutionary processes in the genesis of variably enriched alkaline magmas. *J. Volcanol. Geotherm. Res.*, **75**, 107-136.

Cox, K.G. (1980): A model for flood basalt volcanism. *J. Petrol.*, **21**, 629-650.

Crawford, A.J. (1980): A clinoenstatite-bearing cumulative olivine pyroxenite from Howqua, Victoria. *Contrib. Mineral. Petrol.*, **75**, 353-367.

– (1989): "Boninites". Unwin-Hyman, London, 465 pp.

Di Battistini, G., Montanini, A., Vernia, L., Bargossi, D.G., Gastotina, F. (1999): Petrology and geochemistry of ultrapotassic rocks from the Montefiascone volcanic complex (Central Italy), magmatic evolution and petrogenesis. *Lithos*, **43**, 169-195.

Dobosi, D. & Fodor, R.V. (1992): Magma fractionation, replenishment, and mixing as inferred from green-core clinopyroxenes in Pliocene basanite, southern Slovakia. *Lithos*, **28**, 133-150.

Duda, A. & Schmincke, H.-U. (1985): Polybaric differentiation of alkali basaltic magmas: evidence from green-core clinopyroxenes (Eifel, FRG). *Contrib. Mineral. Petrol.*, **91**, 340-153.

Farnetani, C.G., Richards, M.A., Ghiorso, M.S. (1996): Petrological models of magma evolution and deep crustal structure beneath hotspots and flood basalts. *Earth Planet. Sci. Lett.*, **143**, 81-94.

Francis, D. (1985): The Baffin Bay lavas and the value of picrites as analogues of primary magmas. *Contrib. Mineral. Petrol.*, **89**, 144-154.

Gurenko, A.A., Hansteen, T.H., Schmincke, H.-U. (1996): Evolution of parental magmas of Miocene shield basalts of Gran Canaria (Canary Islands): constraints from crystal, melt and fluid inclusions in minerals. *Contrib. Mineral. Petrol.*, **124**, 422-435.

Holm, P.M. (1982): Mineral chemistry of potassic lavas of the Vulsini district. The Roman province. *Mineral. Mag.*, **46**, 379-386.

Jaques, A.L., Lewis, J.D., Gregory, G.P., Ferguson, J., Smith, C.B., Chappell, B.W., McCulloch, M.T. (1984): The diamond-bearing ultrapotassic (lamproitic) rocks from the west Kimberley region, Western Australia. *In* "Proceedings of the third International Kimberlite Conference", J. Kornprobst, ed., Elsevier, New York, 225-254.

Jurewich, A.J. & Watson, E.B. (1988): Cations in olivine, part 1: calcium partitioning and calcium-magnesium distribution between olivines and coexisting melts, with petrological applications. *Contrib. Mineral. Petrol.*, **99**, 176-185.

Kamenetsky, V., Metrich, N., Cioni, R. (1995): Potassic primary melts of Vulsini (Roman Province): evidence from mineralogy and melt inclusions. *Contrib. Mineral. Petrol.*, **120**, 186-196.

Kelemen, P. & Holbrook, S. (1995): Origin of thick, high-velocity igneous crust along the U. S. East Coast margin. *J. Geophys. Res.*, **100**, 10077-10094.

Korenaga, J., Holbrook, S., Kent, G., Kelemen, P., Detrick, R., Larsen, H-C., Hopper, J., Dahl-Jensen, T. (2000): Crustal structure of the southeast Greenland Margin from joint refraction and reflection seismic tomography. *J. Geophys. Res.*, **105**, 21591-21614.

Larsen, L.M. & Pedersen, A.K. (2000): Processes in high-Mg, high-T magmas: evidence from olivine, chromite and glass in Palaeogene picrites from West Greenland. *J. Petrol.*, **41**, 1071-1098.

Le Bas, M.J. (1962): The role of aluminium in igneous clinopyroxene with relation to their parentage. *Am. J. Sci.*, **260**, 267-288.

Leloup, H., Laccassin, R., Tapponnier, P., Scharer, U., Zhong, D.L., Liu, X. Zhang, L.S., Ji, S., Phan, T.T. (1995): The Ailao Shan-Red River shear zone (Yunnan, China), Tertiary transform boundary of Indochina. *Tectonophysics*, **251**, 3-84.

Li, J.P., O'Neil, H.St., Seifert, F. (1995): Subsolidus phase relations in the system MgO-SiO_2-Cr-O in equilibrium with metallic Cr, and their significance for the petrochemistry of chromium. *J. Petrol.*, **36**, 107-132.

Liu, J., Liu, F., He, J., Chen, H., You, Q. (2001): Study of seismic tomography in Panxi palerift area of southwestern China – structural features of crust and mantle and their evolution. *Science in China*, (Series D), **44**, 277-288.

Maaloe, S. & Hansen, B. (1982): Olivine phenocrysts of Hawaiian olivine tholeiite and oceanite. *Contrib. Mineral. Petrol.*, **81**, 203-211.

Mitchell, R. & Bergman, S.C. (1991): "Petrology of lamproites". Plenum Press, New York, 447 pp.

Nisbet, E.G., Cheadle, M.J., Arndt, N.T., Bickle, M.J. (1993): Constraining the potential temperature of the Archaean mantle: A review of the evidence from Komatiites. *Lithos*, **230**, 291-307.

Neumann, E.R., Wuff-Pedersen, E., Simonsen, S.L., Pearson, N.J., Marti, J., Mitjacila, J. (1999): Evidence for fractional crystallization of periodically refilled magma chambers in Tenerife, Canary Islands. *J. Petrol.*, **40**, 1089-1123.

Revillon, S., Arndt, N.T., Hallot, E., Kerr, A.C., Tarney, J. (1999): Petrogenesis of picrites from the Caribbean Plateau and the North Atlantic magmatic province. *Lithos*, **49**, 1-21.

Simkin, K. & Smith, J.V. (1978): Minor element distribution in olivine. *J. Geol.*, **78**, 304-325.

Spence, K.J. & Lindsley, D.H. (1981): A solution model for co-existing iron-titanium oxides. *Am. Mineral.*, **66**, 1189-1201.

Takahashi, E., Uto, K., Schilling, J.G. (1987): Primary magma compositions and Mg/Fe ratios of their mantle residues along Mid Atlantic Ridge 19°N to 73°N. *Technical Report of ISEI, Okayama University, Ser. A*, **9**, 1-14.

Takahashi, N. (1991): Origin of three peridotite suites from Horoman peridotite complex, Hokkaido, Japan: melting, melt segregation and solidification processes in the upper mantle. *J. Min. Petr. Econ. Geol.*, **86**, 199-215.

Tapponnier, P., Peltzer, G., Armijo, R., Le Dain, A.Y., Cobbold, P. (1982): Propagating extrusion tectonic in Asia: New insights from simple experiments with plasticine. *Geology*, **10**, 611-616.

Thompson, G., Ali, J.R., Song, X.Y., Lolley, D.W. (2001): Emeishan basalts, SW China: reappraisal of the formation's type area stratigraphy and a discussion of its significance as a large igneous province. *J. Geol. Soc. London*, **158**, 591-599.

Thompson, R.N. & Gibson, S.A. (2000): Transient high temperatures in mantle plume heads inferred from magnesian olivines in Phanerozoic picrites. *Nature*, **407**, 502-506.

Trumbell, R.B., Sobolev, S.V., Bauer, K. (2002): Petrophysical modeling of high seismic velocity crust at the Namibian volcanic margin. *In* "Volcanic Rifted Margins", M.A. Menzies, S.L., Klemperer, C.J. Ebinger, J. Baker, eds., Geological Society of America Special Paper **362**, 225-234.

Ulmer, P. (1989): The dependence of the Fe^{2+}-Mg cations-partitioning between olivine and basaltic liquid on pressure, temperature and composition, an experimental study to 30 kbars. *Contrib. Mineral. Petrol.*, **101**, 261-273.

Walker, D.A. & Cameron, W.E. (1988): Boninitic primary magmas: evidence from Cape Vogel Peninsula, PNG. *Contrib. Mineral. Petrol.*, **83**, 150-158.

Wang, X., Metcalfe, I., Jian, P., He, L., Wang, C. (2000): The Jinshajiang-Ailaoshan Suture Zone, China: tectonostratigraphy, age and evolution. *J. Asian Earth Sci.*, **18**, 675-690.

Wass, S.Y. (1979): Multiple origins of clinopyroxenes in alkali basaltic rocks. *Lithos*, **12**, 115-132.

White, R.S. & McKenzie, D. (1989): Magmatism at rift zone: the generation of volcanic continental margins and flood basalts. *J. Geophys. Res.*, **94**, 7685-7729.

Xie, Y. & Zhang, Y. (1995): Petrochemistry of the Cenozoic magmatic rocks in eastern Erhai, Yunnan Province. *Acta Petrologica Sinica*, **11**, 423-433 (in Chinese with English abstract).

Xu, Y.G. & Chung, S.L. (2001): Emeishan large igenous province: evidence for mantle plume activity and its melting condition. *Geochimica*, **30**, 1-9 (in Chinese with English abstract).

Xu, Y.G., Chung, S.L., Jahn, B.M., Wu, G.Y. (2001a): Petrological and geochemical constraints on the petrogenesis of the Permo-Triassic Emeishan Flood basalts in southwestern China. *Lithos*, **58**, 145-168.

Xu, Y.G., Menzies, M.A., Thirlwall, M.F., Xie, G.H. (2001b): Exotic lithosphere beneath the Western Yangtze Craton: Petrogenetic links to Tibet using highly magnesian ultrapotassic rocks. *Geology*, **39**, 863-866.

Yang, T., Cheng, Y., Wang, H. (1986): "The Geology of China". Clarendon Press, Oxford, 303 pp.

Received 11 January 2002
Modified version received 23 September 2002
Accepted 19 May 2003